NASA/TM-2004-213253
ARL-TR-3266

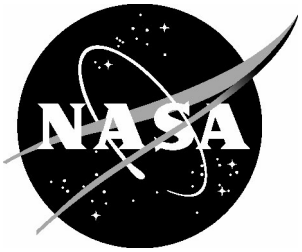

A Comparison of Weld-Repaired and Base Metal for Inconel 718 and CRES 321 at Cryogenic and Room Temperatures

John A. Newman
U.S. Army Research Laboratory
Vehicle Technology Directorate
Langley Research Center, Hampton, Virginia

Stephen W. Smith
Langley Research Center, Hampton, Virginia

Scott A. Willard
Lockheed Martin Engineering and Sciences
Langley Research Center, Hampton, Virginia

Robert S. Piascik
Langley Research Center, Hampton, Virginia

August 2004

The NASA STI Program Office . . . in Profile

Since its founding, NASA has been dedicated to the advancement of aeronautics and space science. The NASA Scientific and Technical Information (STI) Program Office plays a key part in helping NASA maintain this important role.

The NASA STI Program Office is operated by Langley Research Center, the lead center for NASA's scientific and technical information. The NASA STI Program Office provides access to the NASA STI Database, the largest collection of aeronautical and space science STI in the world. The Program Office is also NASA's institutional mechanism for disseminating the results of its research and development activities. These results are published by NASA in the NASA STI Report Series, which includes the following report types:

- TECHNICAL PUBLICATION. Reports of completed research or a major significant phase of research that present the results of NASA programs and include extensive data or theoretical analysis. Includes compilations of significant scientific and technical data and information deemed to be of continuing reference value. NASA counterpart of peer-reviewed formal professional papers, but having less stringent limitations on manuscript length and extent of graphic presentations.

- TECHNICAL MEMORANDUM. Scientific and technical findings that are preliminary or of specialized interest, e.g., quick release reports, working papers, and bibliographies that contain minimal annotation. Does not contain extensive analysis.

- CONTRACTOR REPORT. Scientific and technical findings by NASA-sponsored contractors and grantees.

- CONFERENCE PUBLICATION. Collected papers from scientific and technical conferences, symposia, seminars, or other meetings sponsored or co-sponsored by NASA.

- SPECIAL PUBLICATION. Scientific, technical, or historical information from NASA programs, projects, and missions, often concerned with subjects having substantial public interest.

- TECHNICAL TRANSLATION. English-language translations of foreign scientific and technical material pertinent to NASA's mission.

Specialized services that complement the STI Program Office's diverse offerings include creating custom thesauri, building customized databases, organizing and publishing research results ... even providing videos.

For more information about the NASA STI Program Office, see the following:

- Access the NASA STI Program Home Page at ***http://www.sti.nasa.gov***

- E-mail your question via the Internet to help@sti.nasa.gov

- Fax your question to the NASA STI Help Desk at (301) 621-0134

- Phone the NASA STI Help Desk at (301) 621-0390

- Write to:
  NASA STI Help Desk
  NASA Center for AeroSpace Information
  7121 Standard Drive
  Hanover, MD 21076-1320

NASA/TM-2004-213253
ARL-TR-3266

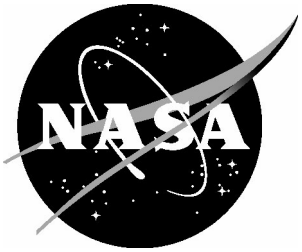

A Comparison of Weld-Repaired and Base Metal for Inconel 718 and CRES 321 at Cryogenic and Room Temperatures

John A. Newman
U.S. Army Research Laboratory
Vehicle Technology Directorate
Langley Research Center, Hampton, Virginia

Stephen W. Smith
Langley Research Center, Hampton, Virginia

Scott A. Willard
Lockheed Martin Engineering and Sciences
Langley Research Center, Hampton, Virginia

Robert S. Piascik
Langley Research Center, Hampton, Virginia

National Aeronautics and
Space Administration

Langley Research Center
Hampton, Virginia 23681-2199

August 2004

Available from:

NASA Center for AeroSpace Information (CASI)
7121 Standard Drive
Hanover, MD 21076-1320
(301) 621-0390

National Technical Information Service (NTIS)
5285 Port Royal Road
Springfield, VA 22161-2171
(703) 605-6000

Abstract

Fatigue crack growth tests were conducted to characterize the performance of Inconel 718 and CRES 321 welds, weld heat-affect-zone and parent metal at room temperature laboratory air and liquid nitrogen (-196°C) environments. The results of this study were required to predict the damage tolerance behavior of proposed orbiter main engine hydrogen fuel liner weld repairs. Experimental results show that the room and cryogenic temperature fatigue crack growth characteristics of both alloys are not significantly degraded by the weld repair process. However, both Inconel 718 and CRES 321 exhibited lower apparent toughness within the weld repair region compared to the parent metal.

Introduction

Fatigue cracks were found during the inspection of orbiter main engine liquid hydrogen feed line flow liners. The flow liner prevents turbulent flow in the flexible bellow joint region, shown in Figure 1a, as liquid hydrogen is pumped into the orbiter main engines. A portion of the inside surface of the upstream and downstream flow liners and their slotted configuration is shown in Figure 1b. The flow liner fatigue cracks initiated at the slots and propagated in either the longitudinal or radial directions. Figure 2 is a photograph of a typical radial crack; here the radial crack propagated 0.3255 inch from the edge of the slot. Small fatigue cracks were found in the flow liners of four orbiters containing either Inconel 718 or CRES 321 flow liners. Refer to Table 1.

Table 1. Orbiter Flow Liner Alloys

Orbiter	Flow Liner Alloy
OV 102	CRES 321
OV 103	Inconel 718
OV 104	Inconel 718
OV 105	Inconel 718

Marshall Space Flight Center (MSFC) developed the flow liner weld repair process in which cracks are repaired by welding the crack faces together. As part of the flow liner repair qualification, it was critical to understand the fatigue crack growth characteristics of the weld-repaired components relative to the original condition. The aim of this study was to characterize and compare the fatigue crack growth properties of the MSFC weld repair and parent material at both cryogenic and room temperatures.

Materials

Inconel 718 (a nickel-base alloy) and CRES 321 (a stainless steel) flow liners are constructed from sheet material having a nominal thickness of 1.27 mm (0.050 inch). Sheet products of each material, approximately 300 mm by 200 mm (12 inch by 8 inch), were provided by MSFC. MSFC also supplied welded specimens that were produced by sectioning a sheet into two pieces (each approximately 300 mm

by 100 mm) and rejoining them using the same welding procedures developed for the weld repair of the orbiter flow liner.

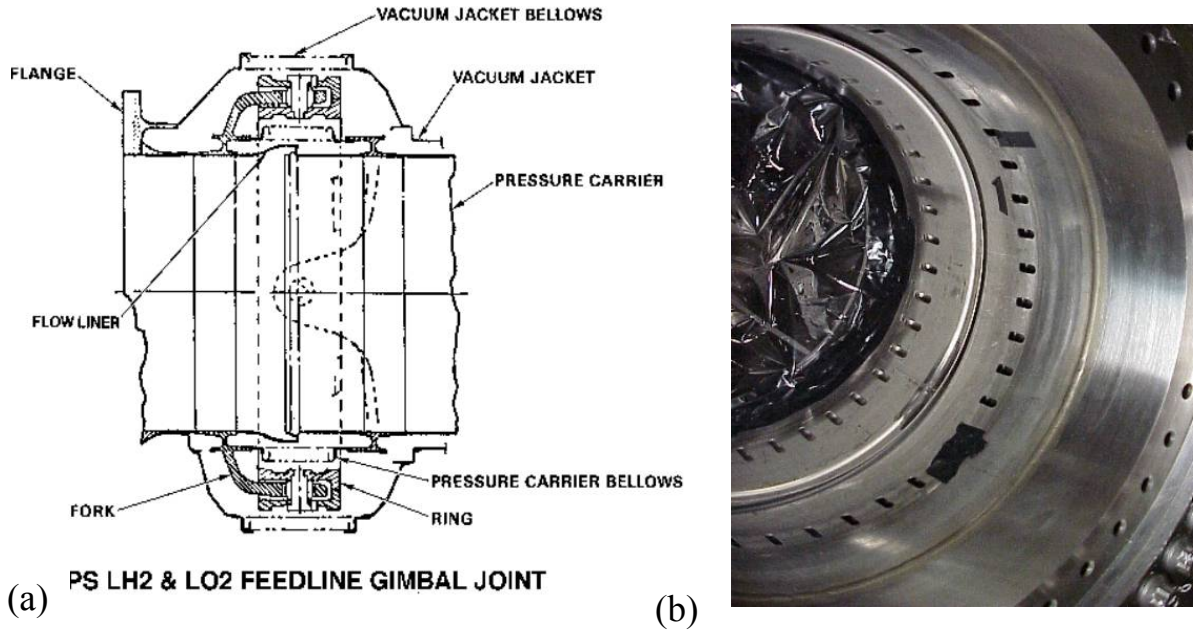

Figure 1. (a) The liquid hydrogen line joint and the location of the flow liner. (b) The inside of the joint and the slotted flow liner configuration.

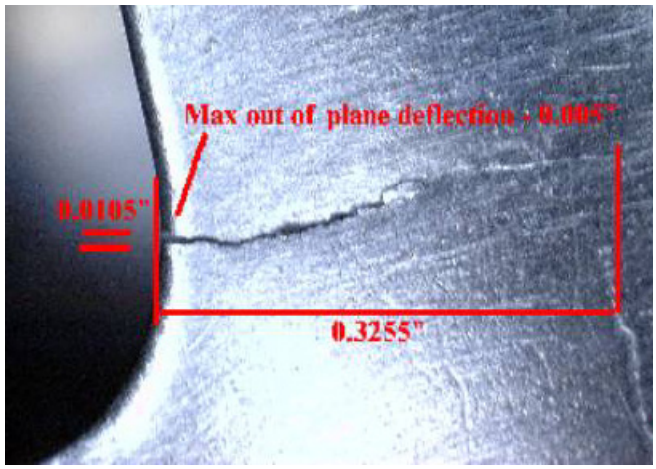

Figure 2. A region of the flow liner inside surface and a typical radial crack found in a flow liner. The crack initiated at a flow liner slot (left side of the photograph) and propagated to a length of 0.3255 inch.

Prior to fatigue crack growth (FCG) testing, both Inconel 718 and CRES 321 weld samples were sectioned perpendicular to the weld and metallographically characterized to determine the configuration of the weld metal and heat-affected zone (HAZ). Based on these data, FCG specimens were fabricated so that the fatigue crack growth characteristics of the entire weld region (weld metal, weld metal HAZ boundary, and HAZ) would be determined. The cross-section was polished and etched to highlight the weld metal and HAZ regions, and micro-hardness measurements were obtained along the sheet mid-thickness. A micrograph of the weld cross-section and the corresponding hardness values for Inconel 718

are shown in Figure 3. The weld metal appears as a dark region in the center of the micrograph. The width of the weld metal is not constant through the sheet thickness; the weld metal is significantly wider at the top of the figure (approximately 3.8 mm) than at the bottom (approximately 2.7 mm). The top of the weld shown in Figure 3 is the surface from which weld heat was applied. The boundary between the HAZ and the base metal can be seen in the micrograph as a subtle texture change (in comparison to the weld/HAZ boundary), which corresponds to a significant change in hardness values approximately 3.8 mm from either side of the weld center. Based on the metallography and hardness results, fatigue crack growth test specimens were machined so that starter notches were placed at one of three locations: (1) the centerline of the weld, (2) the weld/HAZ boundary (offset 1.82 mm from the weld center), or (3) in the HAZ region (offset 2.84 mm from the weld center).

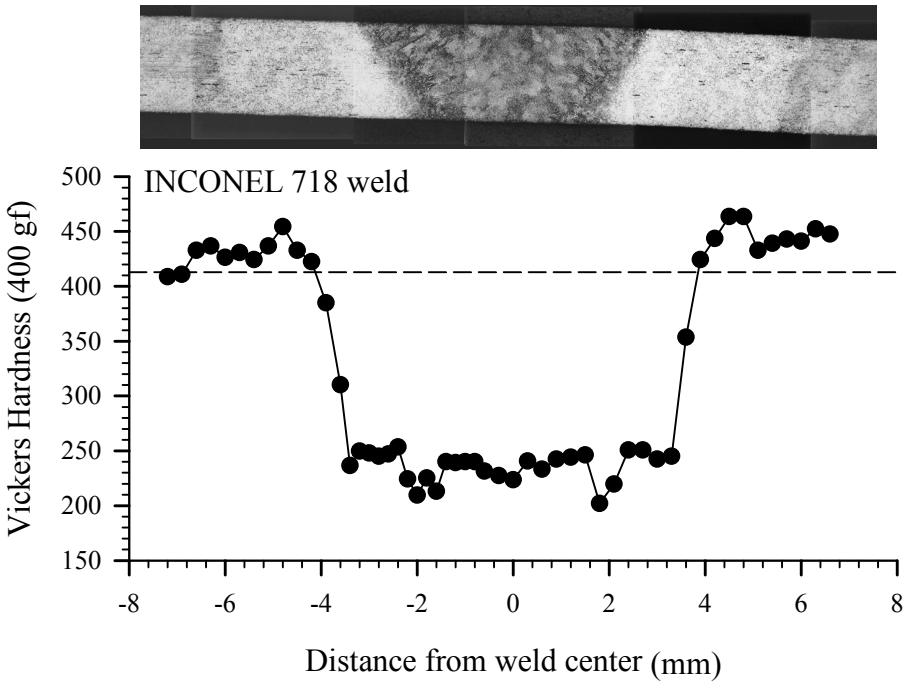

Figure 3. Micrographs and the corresponding hardness values for weld cross-sections of Inconel 718.

A cross-sectional micrograph of a typical CRES 321 weld region, and the corresponding micro-hardness data are shown in Figure 4. The boundary between the weld metal and the HAZ can be seen as a texture change in the micrograph, but no boundary between the HAZ and base metal can be visually detected. Unlike the Inconel 718 results, no significant change in hardness occurs across the weld region so the boundary between the HAZ and base metal cannot be determined. Because the CRES 321 weld was approximately the same size as the Inconel 718 weld, it is assumed that the HAZ dimension would also be similar. Therefore, crack starter notches for CRES 321 specimens are offset from the notch center by the same dimensions as the Inconel 718 specimens: (1) weld center, (2) 1.82 mm from the weld center, or (3) 2.84 mm from the weld center.

Experimental Procedures

Fatigue crack growth tests were performed using computer-controlled servo-hydraulic test machines in accordance with ASTM standard E647 (ref. 1). Tests were performed in either a room-temperature (18–

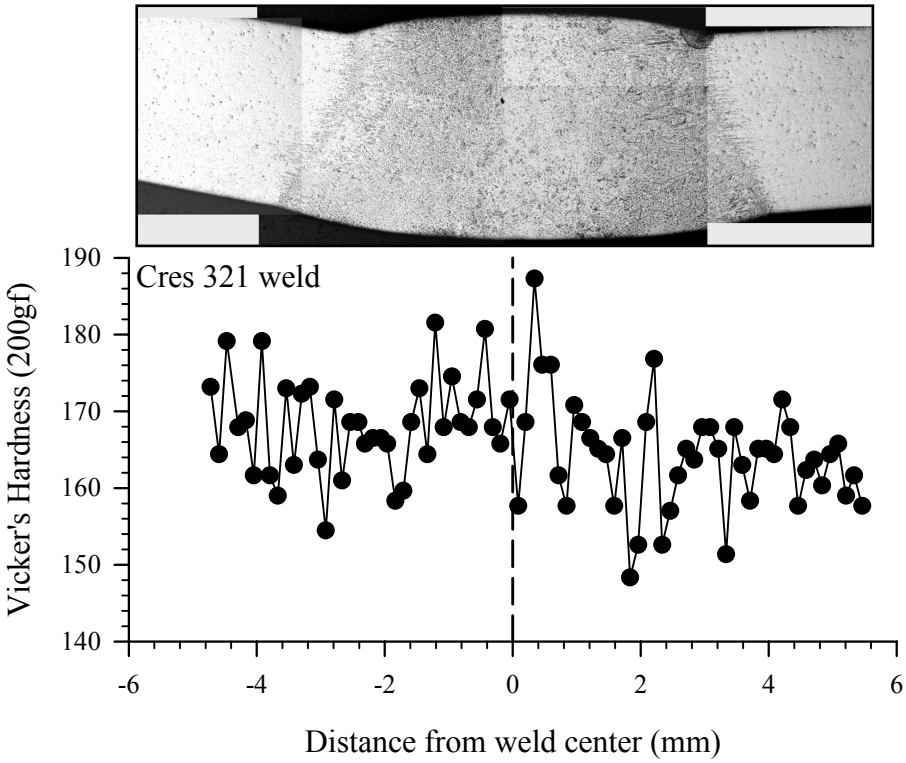

Figure 4. Micrographs and the corresponding hardness values for weld cross-sections of CRES 321.

24°C) laboratory air environment or submerged in liquid nitrogen at -196°C (-320°F).[1] Compliance data were used to monitor crack length during tests, and loads were continuously adjusted to achieve programmed stress-intensity factors (ref. 2). Eccentrically loaded single-edge notch tension (ESET) specimens of width W = 38.1 mm were fabricated in the longitudinal-transverse (L-T) sheet orientation (ref. 3). Specimens were pin loaded as schematically shown in Figure 5. It should be noted that compliance based crack length determinations were verified with visual crack length measurements taken to obtain the initial and final crack length values for each ambient and cryogenic test. After each test, small adjustments (<2%) were made to the compliance-based data based on the visual crack length measurements.

Two-fatigue crack growth rate (FCGR) test methods were used, a constant-K_{max} and constant-stress-ratio (R) test procedure (ref. 1). The constant-R tests were only conducted in room temperature laboratory air because it required an excessive amount of time (30-45 days) to determine the near-threshold FCGR characteristics. Therefore, the majority of testing was conducted using the more rapid constant-K_{max} procedure. Because the preferred constant-K_{max} test is a variable stress ratio (R) test and the near-threshold FCG regime is conducted at high R, crack closure effects are avoided and intrinsic (closure free) FCG data are produced. Intrinsic crack growth data insures a direct comparison between

[1] Data supplied by Johnson Space Center showed little difference in the fracture toughness of Inconel 718 at -196°C (-320°F) and the operating temperature of the liquid hydrogen fuel liners, -253°C (-423°F). Based on the fracture toughness data, little difference in fatigue crack growth characteristics was expected between liquid nitrogen and hydrogen temperatures. Therefore, FCG testing was conducted in liquid nitrogen at temperature, -196°C (-320°F).

base metal and weld metal.[2] The constant-K_{max} test procedure is particularly important since crack closure can mask the true (intrinsic) fatigue crack growth characteristic of the material.

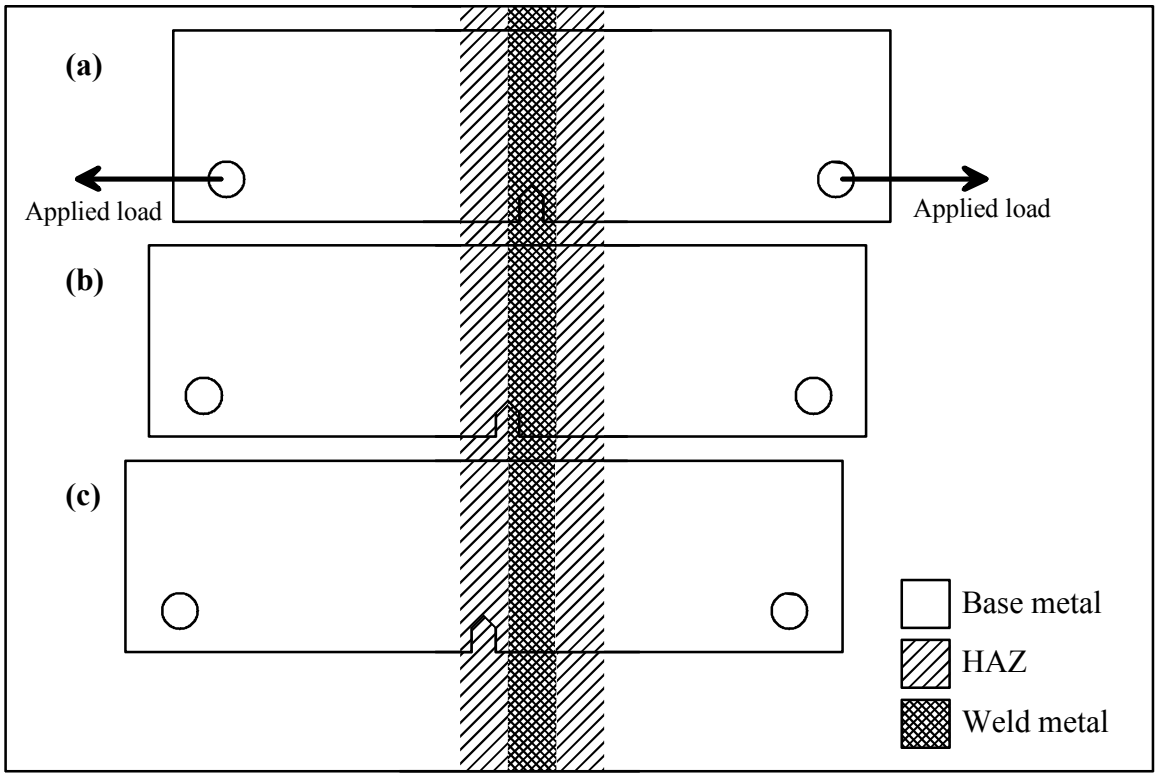

Figure 5. The locations of the crack starter notches are schematically shown: (a) at the weld center, (b) at the interface between the weld metal and HAZ, and (c) in the HAZ.

The FCG specimens were machined from the welded sheets with the crack starter notches parallel to the weld. Crack starter notches were cut in three locations – (1) the weld center, (2) the weld/HAZ boundary, and (3) within the HAZ – as shown schematically in Figure 5. Welds are typically vulnerable to cracking within the heat-affected zone (HAZ) near the weld metal (ref. 6). However, this generalization may not apply to the specific materials (Inconel 718 and CRES 321), sheet thickness (1.27 mm), or test temperatures of interest. Therefore, it was considered prudent to characterize the propagation of fatigue cracks at multiple places within the weld for each material.

Following fatigue crack growth testing, specimens were loaded to failure to characterize the relative material toughness. These toughness tests were not performed in accordance with standard procedures for fracture toughness (*i.e.*, the ESET specimen is not an accepted specimen for fracture toughness testing, consequently constraints on *a*/W and thickness for this specimen have not been specified); therefore, specific fracture toughness values have not been determined. However, these tests do permit a relative comparison to be made between toughness values of the weld metal and base metal specimens.

Additional FCG specimens were machined from a welded Inconel 718 sheet with the weld oriented parallel to the loading axis to obtain FCGR data as the crack propagated normal to the welding direction. It was hoped that these test data would yield a variation in crack growth rate relative to the weld HAZ, the

[2] Using closure-free near-threshold FCG data is preferable to correcting constant-R test FCG data for crack closure by calculating an effective crack-tip driving force. Near-threshold FCG closure determinations are considered subjective and therefore near-threshold effective crack-tip stress intensity factor is inexact (refs. 4 and 5).

weld/HAZ boundary and weld metal; thus identifying regions of accelerated FCG. However, cracks were deflected from the anticipated crack path before reaching the weld region, presumably due to residual stresses within the welded specimens, in both specimens tested. A photograph of a deflected crack is shown in Figure 6. Since a straight crack could not be achieved (crack growth normal to the weld) no further tests were performed with specimens having this weld orientation. Discussions of weld residual stress effects are given later in this document.

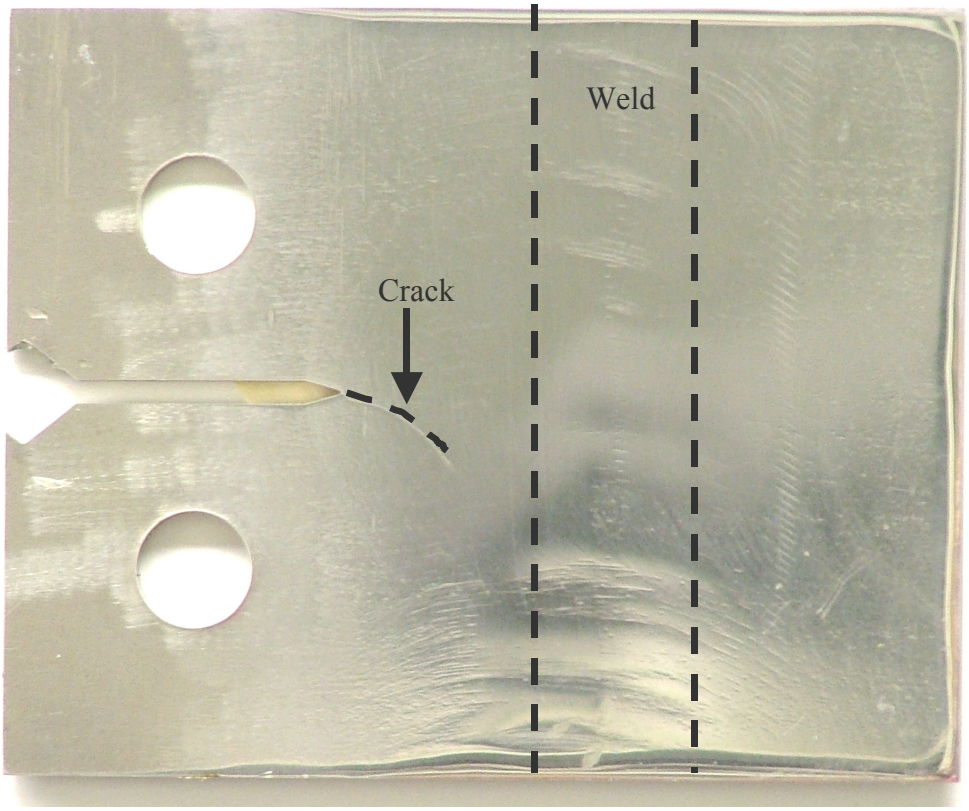

Figure 6. Photograph of a deflected crack in a specimen with anticipated crack path normal to weld.

Fatigue Crack Growth Test Results

Inconel 718 and CRES 321 fatigue crack growth test results are summarized in this section. Testing was conducted to compare the FCG properties of parent metal and weld metal in room temperature laboratory air and liquid nitrogen environments.

INCONEL 718 Results

Room Temperature: The room temperature FCG data for Inconel 718 base metal are plotted in Figure 7a, including three constant-K_{max} conditions (33.0 MPa√m, 66.0 MPa√m, and 132 MPa√m) and two constant-R conditions (0.1 and 0.5). Constant-K_{max} tests were started at relatively high ΔK values and ΔK was continuously reduced as the crack propagated ($C = -787\ m^{-1}$). Constant-R data was obtained by starting tests in the Paris regime (10 MPa√m < ΔK < 20 MPa√m) and either decreasing ($C = -78.7\ m^{-1}$) or increasing ($C = +197\ m^{-1}$) ΔK as the crack propagated. Inconel 718 does not appear to be sensitive to K_{max} effects because no appreciable differences are seen between the three constant-K_{max} data sets. Because constant-K_{max} threshold data are not affected by crack closure, these results suggest that all

appreciable load ratio effects are related to crack closure, and that the constant-K_{max} = 33.0 MPa√m data in Figure 7a represents the closure-free (intrinsic) crack growth behavior for ambient laboratory air.

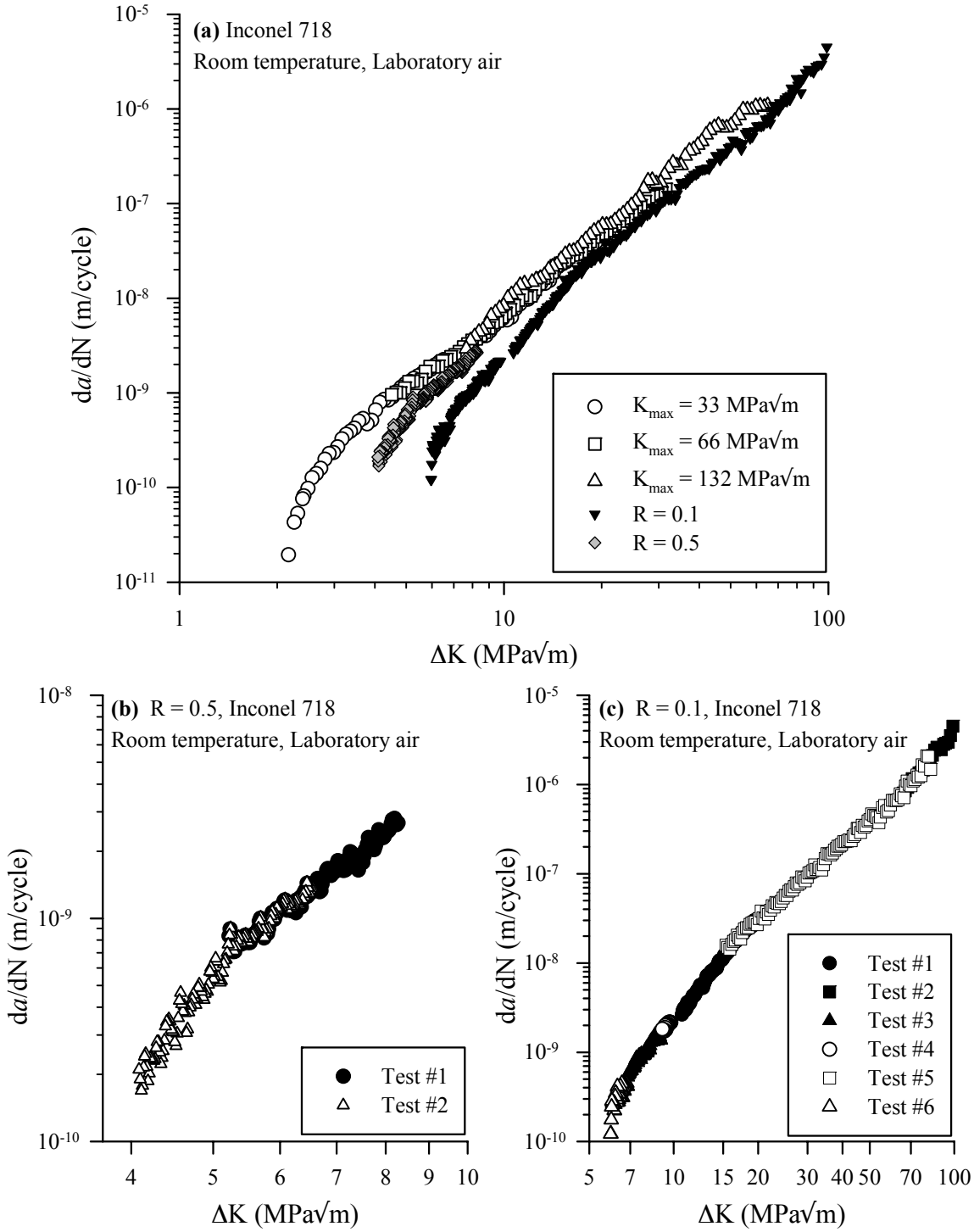

Figure 7. (a) Base-metal room temperature FCG data are shown for Inconel 718. (b) Constant-R = 0.5 data are comprised of two tests. (c) Constant-R = 0.1 data are comprised of six tests.

Tests were repeated to ensure that the results of Figure 7a were reproducible. It is especially important to show reproducibility for constant-R-decreasing-ΔK test results because of the possibility of load history effects (ref. 7). The constant-R = 0.5 and constant-R = 0.1 data shown in Figure 7a are actually comprised of multiple tests, each with a different load history and crack length. The constant-R = 0.5 data consists of two ΔK-decreasing tests (see Figure 7b). The first test (8 MPa√m > ΔK > 5 MPa√m) and second test (6.5 MPa√m > ΔK > 4.1 MPa√m) are in good agreement with each other, suggesting that load history does not affect these data. The constant-R = 0.1 data of Figure 7c consist of six individual tests (three with decreasing ΔK and three with increasing ΔK). The excellent agreement between these sets of data, each with a different load history, suggests that load history does not influence these data. Several constant-K_{max} tests were also repeated (not shown here) with no appreciable differences noted between sets of data. The excellent repeatability of these results strongly suggests that these data are a good measure of the material crack growth behavior and are not influenced by the test method.

The room-temperature FCG data for the welded Inconel 718 specimens are plotted in Figure 8. Tests were performed at constant-K_{max} = 33.0 MPa√m for each of the three starter notch locations. For comparison, the corresponding base-metal data from Figure 7a are also plotted. Only constant-K_{max} = 33.0 MPa√m tests were conducted because the base-metal results showed no K_{max} effect and the FCG threshold was reached without crack closure effects. As seen in the figure, the welded specimens exhibited lower crack growth rates, d*a*/dN, compared to the base metal.

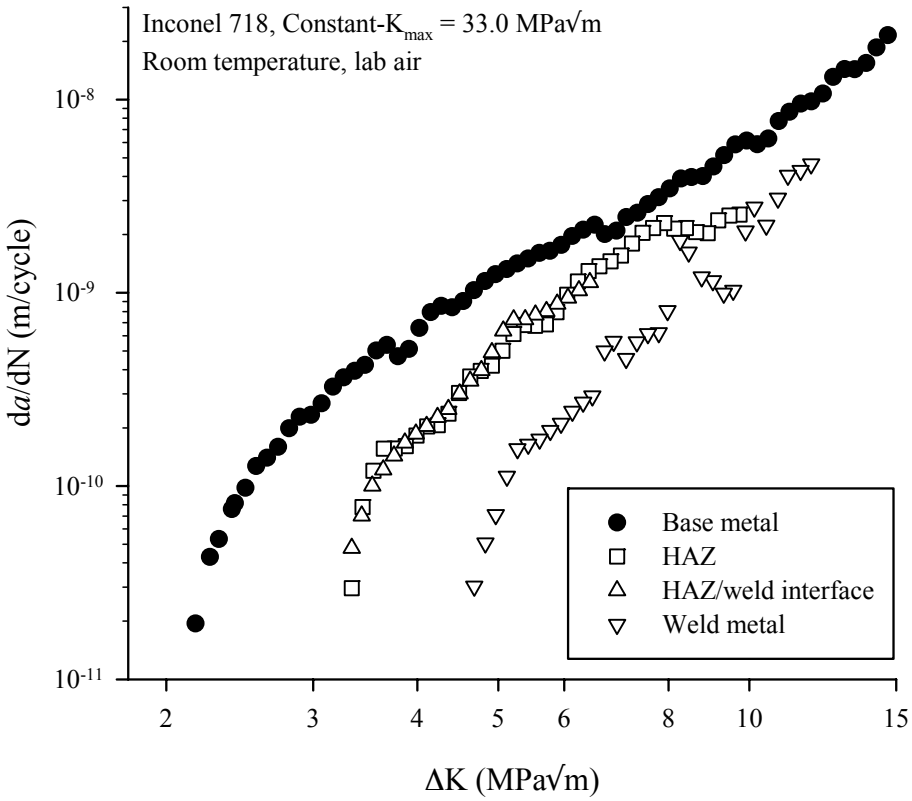

Figure 8. Room temperature FCG data for welded Inconel 718 specimens are shown.

Cryogenic Temperature: Cryogenic FCG data for Inconel 718 base metal are plotted in Figure 9. Due to the complex nature of performing FCG tests submerged in liquid nitrogen, cryogenic testing was kept to a minimum and only constant-K_{max} = 33.0 MPa√m tests were performed. This test was repeated

four times to evaluate the test equipment and to ensure repeatable results. The first three tests were stopped prematurely due to suspected problems with the test equipment. Equipment issues were resolved prior to the fourth test. However, the good agreement between all four sets of data indicates that the first three tests were stopped before equipment problems affected the test data. A comparison of the liquid nitrogen FCG data with the room temperature data (dashed line) in Figure 9 reveals lower FCG rates at cryogenic temperatures. The FCG threshold is approximately 2 MPa√m and 4 MPa√m for room temperature and cryogenic temperature, respectively.

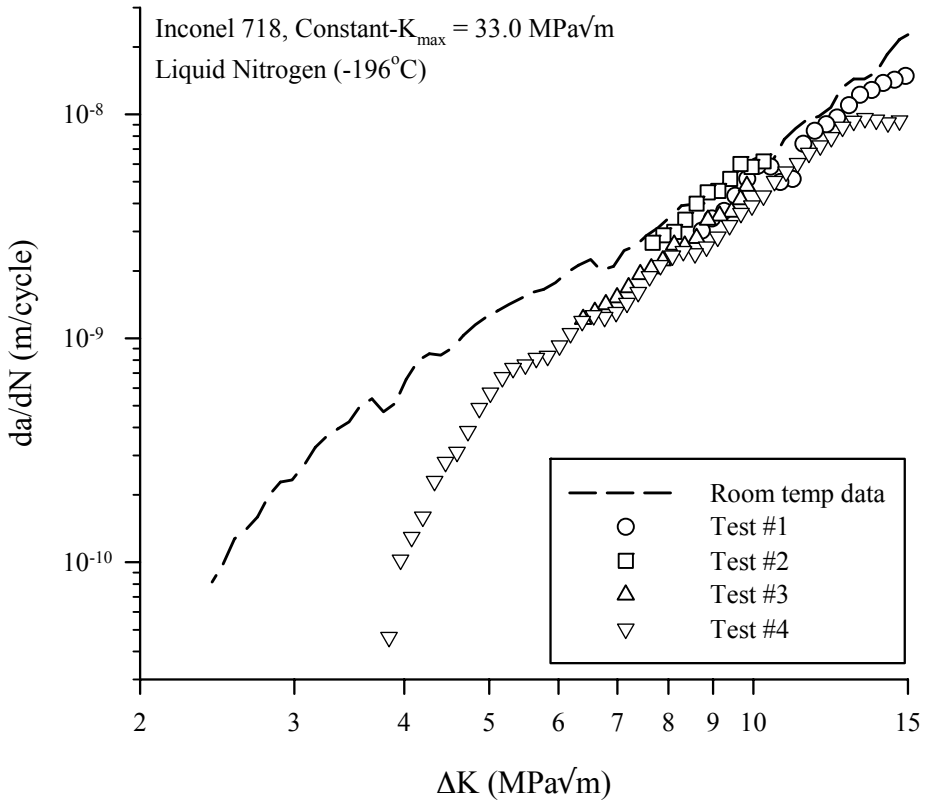

Figure 9. Cryogenic FCG data for Inconel 718 base metal are shown.

The cryogenic FCG data for Inconel 718 welded specimens are compared in Figure 10. As indicated previously, all cryogenic testing for this alloy was performed under constant-K_{max} = 33.0 MPa√m conditions. The corresponding base metal data from Figure 9 are plotted here for comparison. Fatigue crack growth data are not shown for the weld metal because no fatigue crack growth occurred for $\Delta K \leq$ 15 MPa√m in three attempts. A comparison of the base-metal data and the data for the HAZ and the weld/HAZ locations in Figure 10 reveals a lower d*a*/dN for welded specimens compared to that observed in the base metal. This trend is similar to that observed for room temperature air shown in Figure 8. Specifically, the weld specimen data exhibits a ΔK_{th} = 5 MPa√m, significantly higher than the base metal data showing a ΔK_{th} < 4 MPa√m.

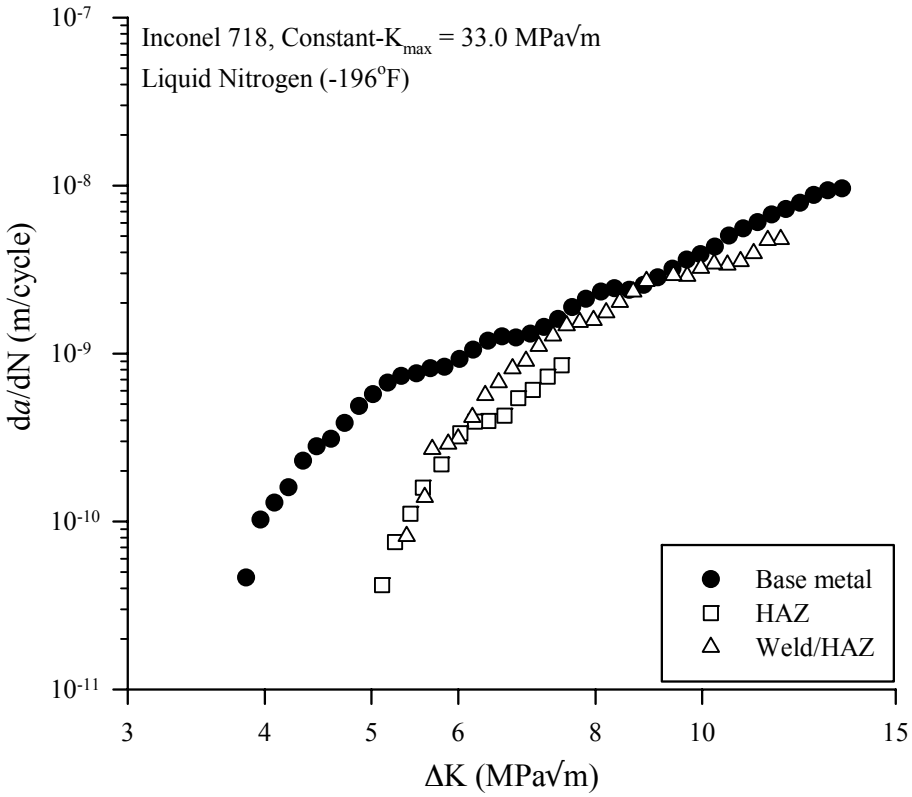

Figure 10. Cryogenic FCG data are shown for welded Inconel 718 specimens.

CRES 321 Test Results

The following paragraphs summarize the fatigue crack growth data for welded and base metal CRES 321 specimens.

Room Temperature: The room temperature FCG data for the CRES 321 base metal are plotted in Figure 11. Test data are shown for three constant-K_{max} conditions (K_{max} = 16.5 MPa√m, 33.0 MPa√m, and 49.5 MPa√m) and constant-R = 0.1. Data for K_{max} = 33.0 MPa√m and 49.5 MPa√m are in good agreement, but the K_{max} = 16.5 MPa√m data show lower crack growth rates. Because this test was started at R = 0.1 and ended at approximately R = 0.7, it is possible that these lower crack growth rates are a result of crack closure. The R = 0.1 data show a similar slope, but with much lower crack growth rates than the other curves. Both the R = 0.1 and K_{max} = 16.5 MPa√m tests were interrupted before achieving near-threshold conditions.

The room-temperature FCG data for the CRES 321 weld specimens are plotted in Figure 12 for constant-K_{max} = 33.0 MPa√m. Unlike the corresponding Inconel 718 data, the CRES 321 weld specimens exhibited slighter higher crack growth rates (less than a factor of 2) compared to the base metal at room temperature.

Cryogenic Temperature: The cryogenic FCG data for the CRES 321 base metal are plotted in Figure 13. Two constant-K_{max} conditions (K_{max} = 16.5 MPa√m, and 33.0 MPa√m) were conducted. Without knowledge of the cryogenic fracture toughness, it was initially feared that K_{max} = 33.0 MPa√m might be approaching the fracture toughness and the resulting fatigue crack growth data might be a poor

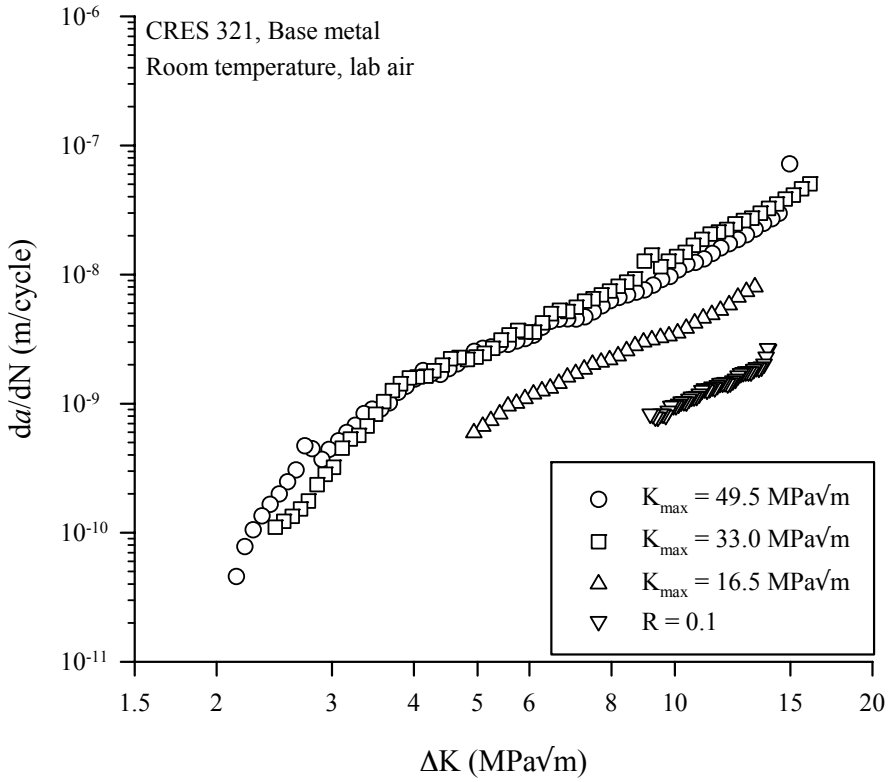

Figure 11. Room temperature FCG data for CRES 321 base metal are shown.

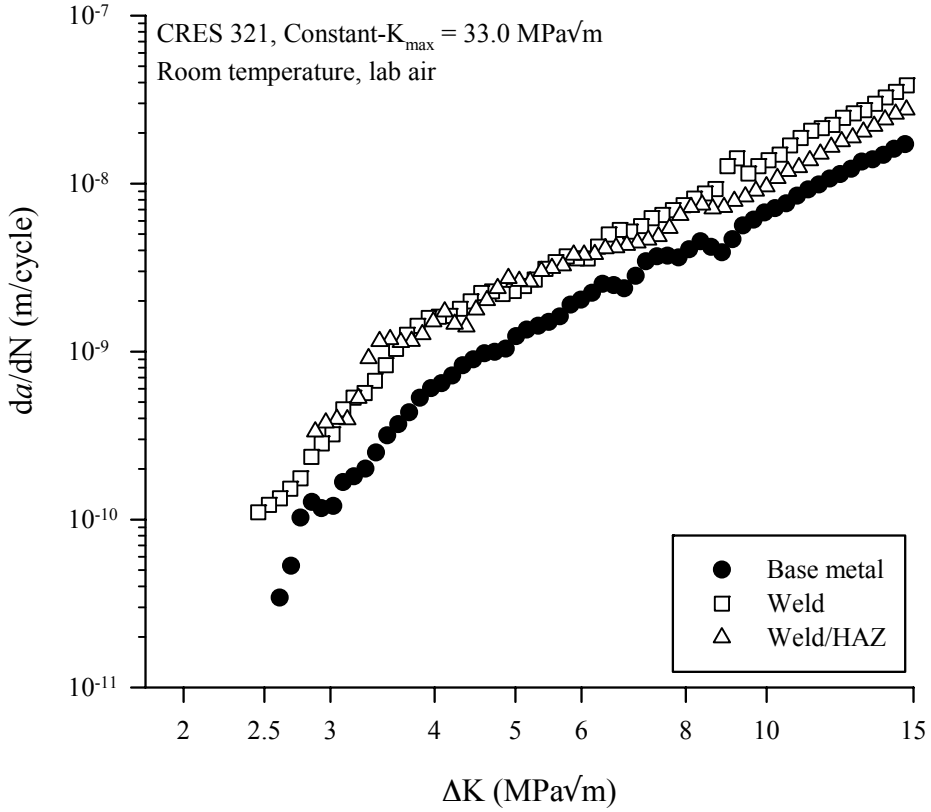

Figure 12. Room temperature FCG data for CRES 321 welded specimens.

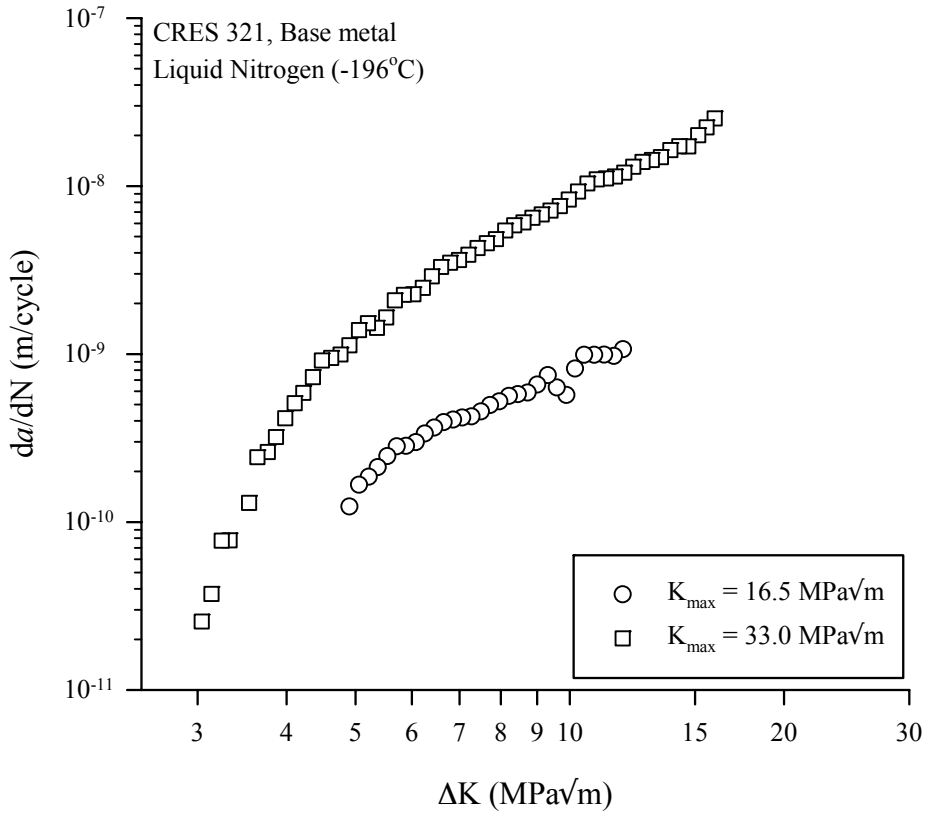

Figure 13. Cryogenic FCG data for CRES 321 base metal

representation of intrinsic crack growth behavior in this alloy. However, it is shown later that K_{max} = 33.0 MPa√m is less than 50% of the specimen apparent toughness at cryogenic temperature. Note that lower crack growth rates were observed during the K_{max} = 16.5 MPa√m test, likely because these data are affected by crack closure. Crack closure is more likely to affect crack growth rates at low R. During the K_{max} = 16.5 MPa√m test, values of R ranged from approximately 0.1 to 0.7. Normally, crack closure is not expected to occur at R > 0.5 unless crack-face roughness or oxides produce atypically high closure levels. Constant-K_{max} = 33.0 MPa√m data are used as a closure-free base line curve because they are not affected by crack closure and the value of K_{max} was significantly less than the fracture toughness.

Cryogenic FCG data for the CRES 321 weld specimens are plotted in Figure 14. These data include two constant-K_{max} conditions (K_{max} = 33.0 MPa√m, and 16.5 MPa√m, shown in Figures 14a and 14b, respectively) for each of the three weld locations and base metal. For K_{max} = 33.0 MPa√m (Figure 14a), the fatigue crack growth data are in good agreement with the base metal results regardless of the location of the crack starter notch. Here, the base metal crack growth rates are, on average, slightly less (approximately 25%) than for the welded specimens. For K_{max} = 16.5 MPa√m (Figure 14b), the base metal data show significantly lower crack growth rates (as much as a factor of 4 lower) relative to the welded specimens. The exaggerated differences between base metal and weld metal specimens is believed to be caused by crack closure, which may affect the K_{max} = 16.5 MPa√m data. However, no additional testing was performed to confirm this. The K_{max} = 33.0 MPa√m is much less likely to be affected by crack closure and is therefore considered a better measure of the intrinsic (closure-free) crack growth behavior. Thus, the fatigue crack growth rates for the base metal are slightly lower, but nearly the same, as for the welded specimens.

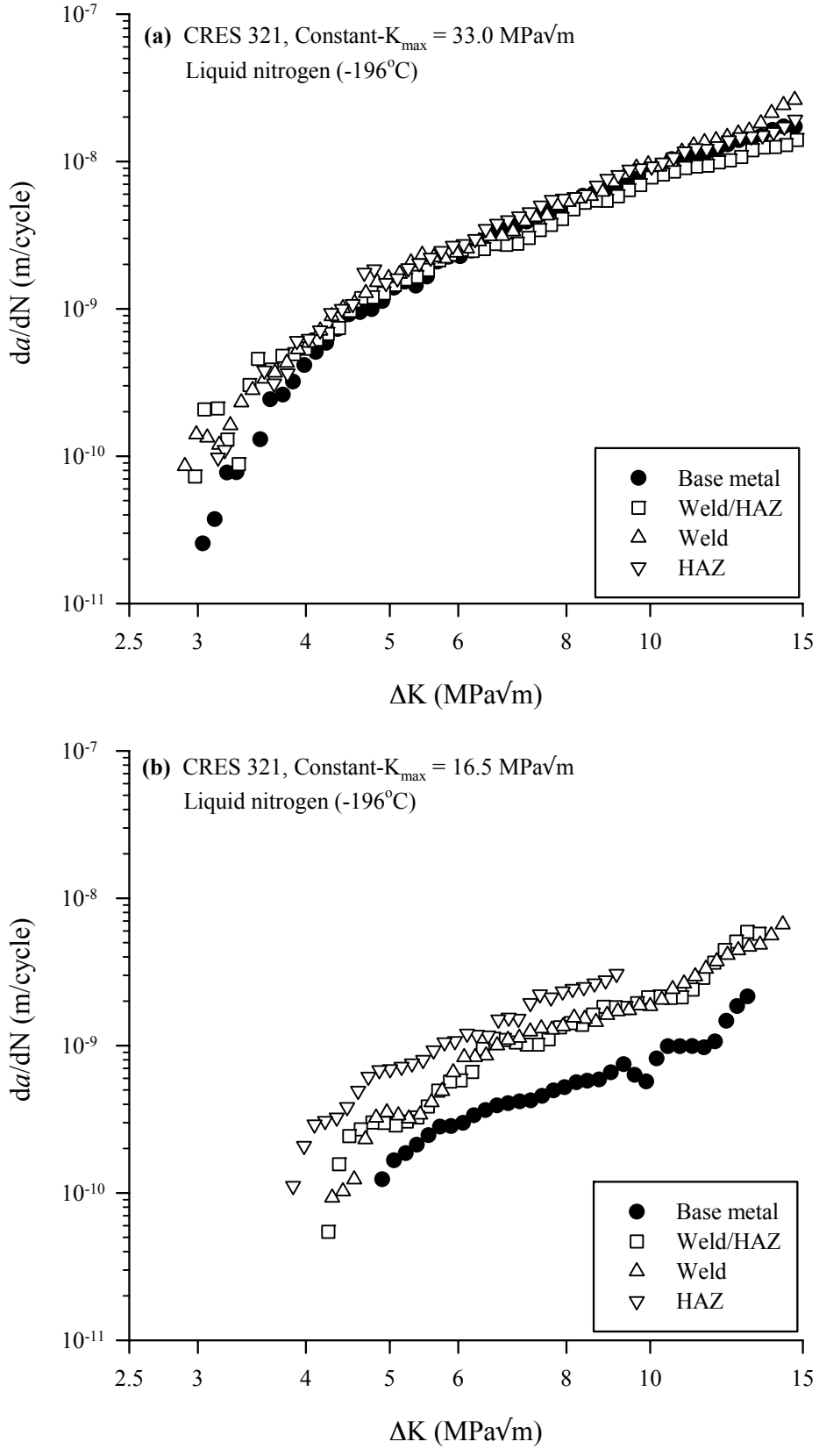

Figure 14. Cryogenic FCG data of CRES 321 weld specimens; (a) K_{max} = 33.0 MPa√m (b) K_{max} = 16.50 MPa√m.

Crack Roughness Characterization

The results of Figures 8 and 10 showed decreasing crack growth rates in Inconel 718 as the crack notch location approached the center of the weld for both test temperatures. For these tests, constant-K_{max} = 33.0 MPa√m testing was performed to avoid crack closure issues at threshold, while keeping K_{max} significantly below the toughness value. No such trend was observed for CRES 321. Closure levels determined from clip gage compliance data indicated no crack closure occurred during the constant-K_{max} tests, however, it has been shown that such far-field compliance methods are not sensitive to near-crack-tip closure events such as roughness-induced crack closure (ref. 5). Therefore, it is possible that the decreasing crack growth rates in the weld metal are a product of roughness-induced crack closure. Further, the possibility that fuel-liner crack bifurcation might release a piece of metal into the flow of cryogenic fuel is a danger because it could cause pump damage. Therefore, it was important to characterize crack roughness and the tendency for crack bifurcation to occur in both the base and weld metal. Photographs of the crack profiles for Inconel 718 specimens are shown in Figures 15 and 16 for constant-K_{max} = 33.0 MPa√m testing at cryogenic and room temperatures, respectively.

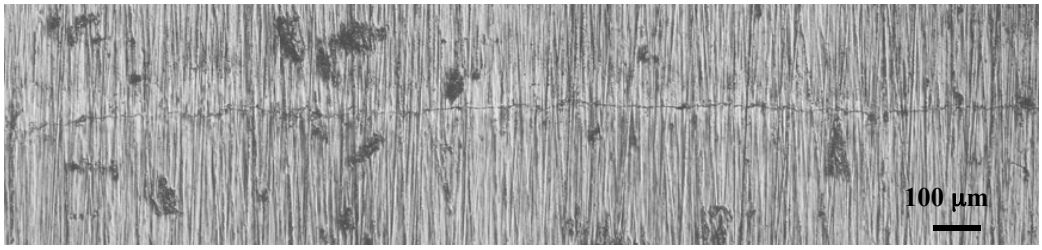

(a) Base metal

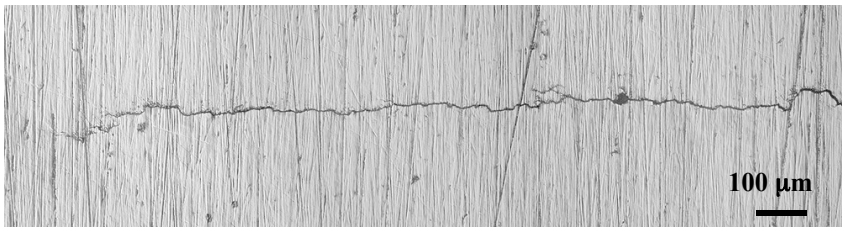

(b) HAZ

(c) HAZ/weld interface

Figure 15. Photographs of crack profiles in Inconel 718 specimens testing at cryogenic temperature.

At cryogenic temperature (-196°C), the crack roughness of the base metal (Figure 15a) and the HAZ (Figure 15b) appear to be similar; both cracks are nominally straight with little or no crack branching, and typical crack-wake asperities are on the order of 10-20 μm in height. The severity of crack-wake roughness appears to be significantly greater at the HAZ/weld interface, as shown in Figure 15c, typical

asperity height is on the order of 40 μm), although no crack branching is observed. Recall from the discussion of Figure 10 that no crack propagation occurred in the center of the weld for these loading conditions (K_{max} = 33.0 MPa√m, $\Delta K \leq$ 16.5 MPa√m).

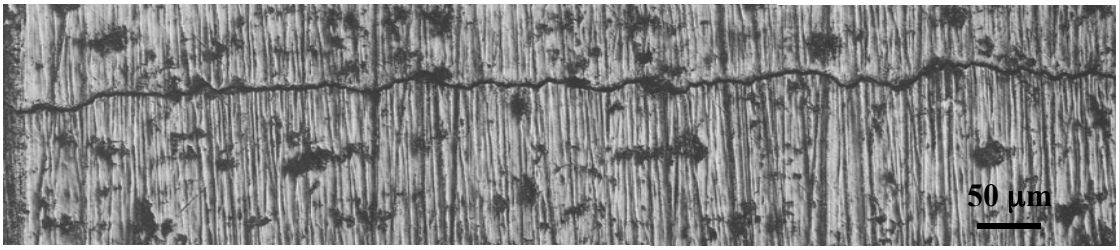

(a) Base metal

(b) HAZ/weld interface

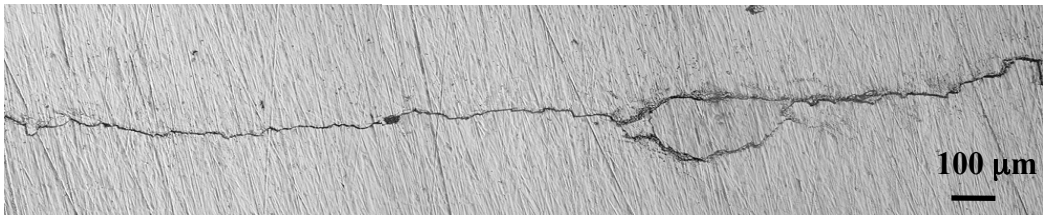

(c) Weld center

Figure 16. Photographs of crack profiles in Inconel 718 specimens testing at ambient temperature.

At room temperature, the crack wake for the base metal (Figure 16a) is nominally straight with little or no crack branching and with a typical asperity height of 10-20 μm. In contrast, the crack-wake for the HAZ/weld interface (Figure 16b) appears to have a slightly higher degree of roughness (typical asperity height of 20-40 μm) and some crack branching is observed. The tendency for crack branching is most prevalent in the weld center (Figure 16c). On the right side of Figure 16c a crack branch appears to have nearly returned to the primary crack, potentially releasing a small (approximately 400 μm by 150 μm) piece of metal. No three-dimensional characterization of this crack branching was done, but this two-dimensional observation suggests that crack bifurcation could be a potential issue in the weld metal. Further, because the severity of crack-wake roughness tends to increase with decreasing distance from the weld center, it is possible that the reduced crack growth rates in the weld metal (recall Figures 8 and 10) could be a result of roughness-induced crack closure that far-field compliance methods are unable to resolve. Although this scenario is considered unlikely, further study is needed to resolve this issue, and the initial assessment of superior intrinsic crack growth resistance for Inconel 718 welded material should be tempered.

Consideration of Residual Stresses

It is known that the welding processes can introduce residual stress effects that influence fatigue crack growth rates. Based on earlier discussions relative to Figure 6, it is presumed that the welded specimens studied here contain significant residual stresses. Limited tests (Inconel 718 only) were conducted in an attempt to assess, but not quantify, the influence of residual stress on fatigue crack growth rates.

Effects of Stress Relieving

Stress relieving – holding the affected material at high temperature for a period of time – may offer a way to reduce the weld-induced residual stresses. The intent of stress relieving is to reduce the residual stresses in the material without adversely affecting base metal properties. To determine the effect of stress relief on base metal FCG rates, compact tension (CT) specimens were fabricated from the base metal and exposed to two stress relieving processes: either 4 hours at 704°C (1300°F) or 8 hours at 816°C (1500°F). Constant-K_{max} = 33.0 MPa√m FCG test data for the two stress-relieved base metal processes are plotted in Figure 17. For comparison, FCG data (K_{max} = 33.0 MPa√m) for the "as received" base metal are also plotted. No significant differences are noted between the FCG data sets in Figure 17, indicating that the stress-relieving processes used here do not significantly influence the fatigue crack growth behavior of the base metal. A hardness survey was performed on the stress-relieved weld samples to determine if the stress-relieving process affects the weld material. The results shown in Figure 18 suggest a significant change in parent and weld metal properties. Here, there is an increase in weld region hardness and reduction in parent metal hardness for the 8 hours at 816°C (1500°F) stress relief process. Even though little difference was noted between the stress-relieved and as-received parent metal FCG rates, the hardness survey strongly suggests that the stress relief process altered parent and weld

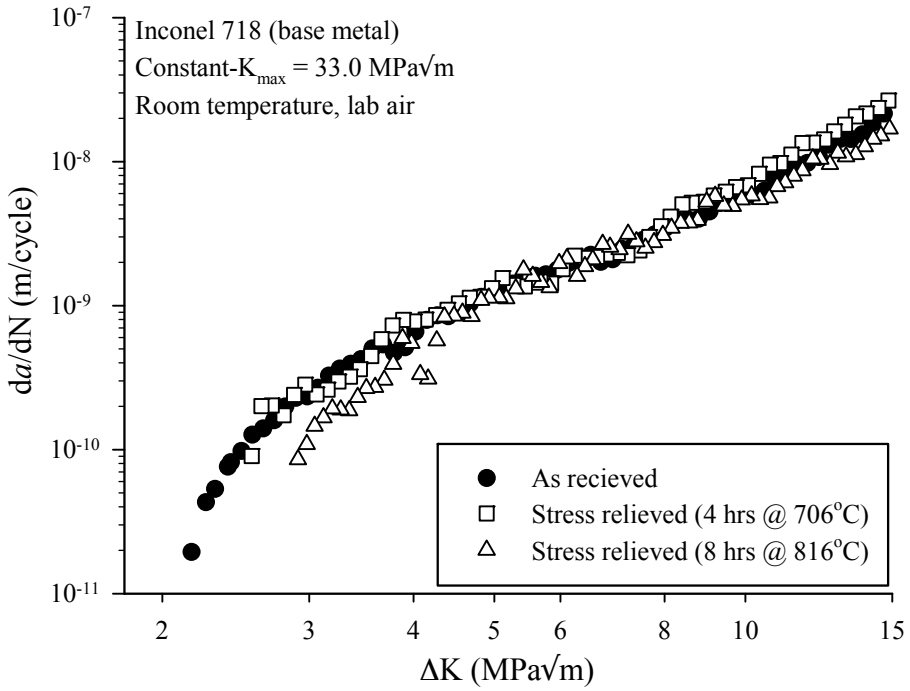

Figure 17. FCG data are shown for stress-relieved Inconel 718 base metal.

metal material properties. No additional FCG tests were conducted on stress relieved weld specimens to quantify the residual stress effects because the stress relief process influences material properties.

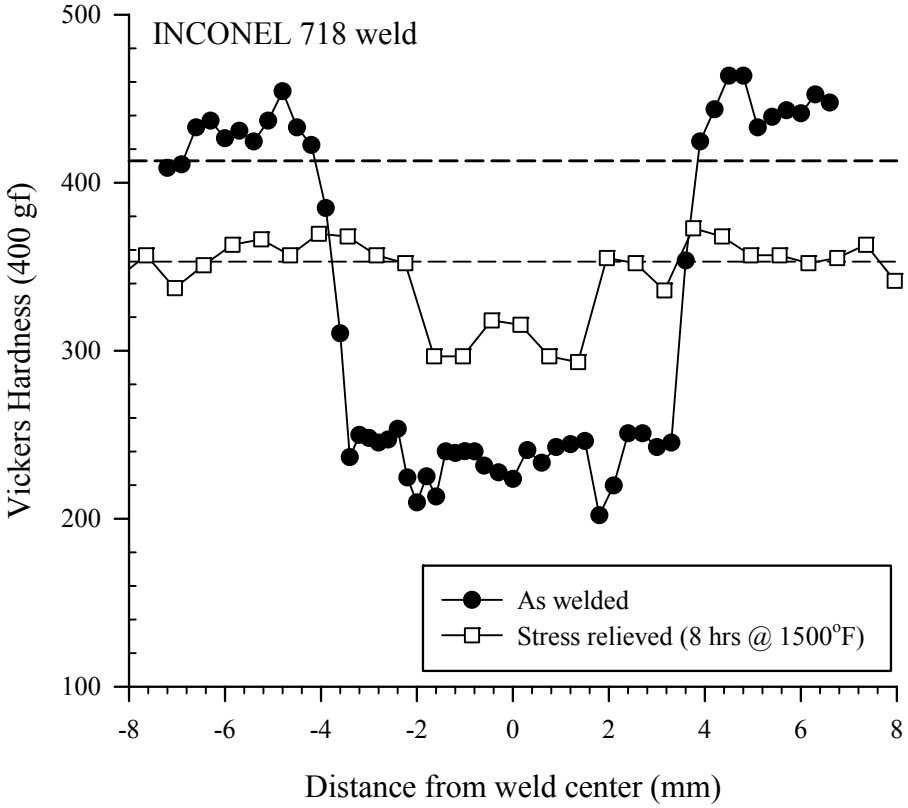

Figure 18. Micro-hardness data of stress-relieved Inconel weld metal.

Evaluation of Weld-induced Residual Stress

An additional test was conducted to indirectly determine the magnitude of the weld-induced residual stresses normal to the crack plane. For crack propagation along the weld line, the redistribution of residual stresses will likely cause specimen deformation that will be detected by back-face strain measurements. The specimen configuration shown in Figure 19 depicts the test using an electro-discharge-machining (EDM) plunge cutter to simulate the fatigue crack. The EDM process cuts a thin, crack-like notch using a highly-localized-heating electric sparking process that limits the introduction of additional residual stresses. As the EDM notch was cut along the HAZ/weld boundary in increments of approximately 1.9 mm (0.075 inch), back-face strain measurements were taken (refer to Figure 19b). The notch length and corresponding back-face strain measurements were obtained after each EDM notch depth increment. This process was repeated until the specimen was cut to a depth of approximately 33 mm (1.3 inches) or an of a/W = 0.65.

When the crack-like notch is produced, residual stresses near the notch are relieved and the internal stresses are redistributed to compensate for the change. This results in strain changes at the specimen back-face. Schindler (ref. 8) has developed a technique to experimentally determine residual stresses, which is used here. According to Schindler, the stress intensity factor due to residual stresses is determined as,

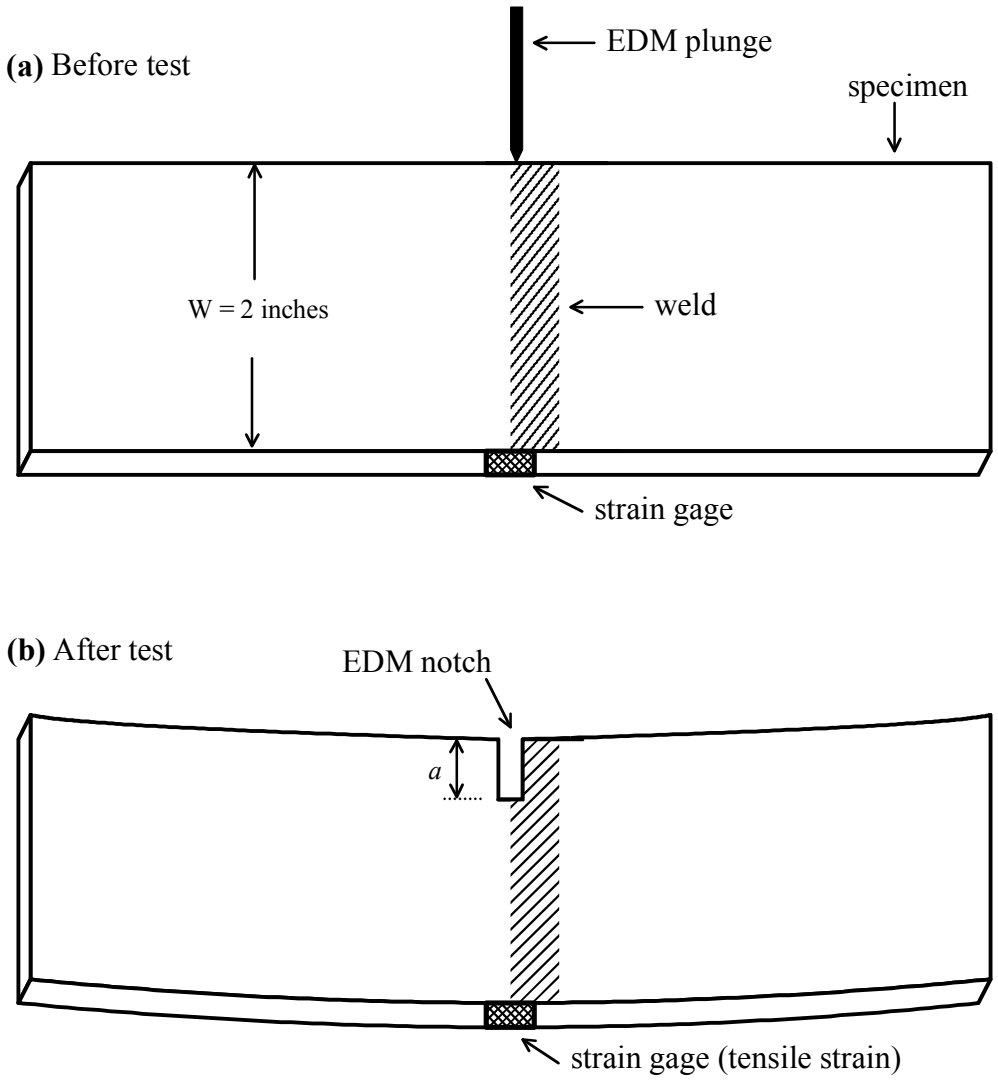

Figure 19. The compliance-cut procedure used to evaluate weld-line residual stresses is schematically depicted. (a) The specimen configuration prior to the test is shown. (b) The specimen configuration after the test is shown. The deformations in (b) are exaggerated for clarity.

$$K_{Irs} = \frac{E'}{Z(a)} \cdot \frac{d\,\varepsilon_M}{da} \tag{1}$$

where ε_M is the back-face strain, E' is the generalized elastic modulus ($E' = E$ for plane stress and $E' = E/(1-\nu^2)$ for plane strain), a is the cut depth, and $Z(a)$ is the influence function. For the specimen configuration used in this study (see Figure 19), the influence function, $Z(a)$ is,

$$Z(a) = \frac{-2.532}{(W-a)^{1.5}} \cdot \sqrt{1-25\left(a/W - 0.2\right)^2} \cdot \left[5.926\left(0.2 - a/W\right)^2 - 0.288\left(0.2 - a/W\right) + 1\right] \tag{2a}$$

for a/W < 0.2 and,

$$Z(a) = \frac{-2.532}{(W - a)^{1.5}} \tag{2b}$$

for 0.2 < a/W < 1. Note that the procedure was developed for crack closure scenarios, and only considers residual stresses that result in opening mode (mode I) stress intensity states. For this study the weld-induced residual stresses are assumed to be primarily mode I in nature. However, this assumption may not be strictly true, since the weld is not uniform through the sheet thickness, as shown in Figures 3 and 4.

The results of Inconel 718 test are shown in Figure 20 as back-face strain versus EDM cut depth. The back-face strain values increase in a near linear manner with increasing EDM cut depth. Note that the strain values are positive, meaning that the specimen deforms as depicted in Figure 19b and the residual stresses normal to the EDM cut are compressive. Following the procedure outlined by Schindler (ref. 4), the corresponding (mode-I) stress intensity values are plotted in Figure 21. (Plane strain conditions were assumed.) The K_{Irs} values have neither an increasing or decreasing trend with respect to depth of cut, and having a typical value of K_{Irs} = -0.2 MPa√m, where the negative value indicates a compressive crack-tip stress. The contributions of the residual stresses to the crack-tip stress state are small. This residual stress contribution will only influence mean-stress. In other words, the actual K_{max} value at the crack tip is slightly larger than applied, but the cyclic stress intensity factor (*i.e.*, ΔK) is not affected by the residual stresses. In the case of a constant-K_{max} = 33.0 MPa√m test, the actual K_{max} value would be approximately 32.8 MPa√m (a decrease of 0.6%).

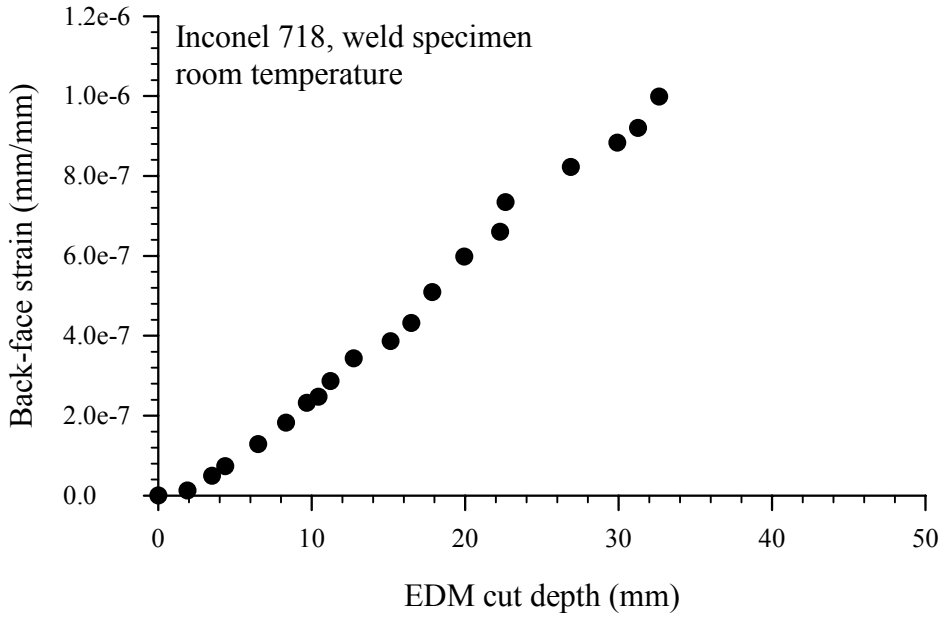

Figure 20. Back-face-strain versus EDM-cut-depth results are plotted.

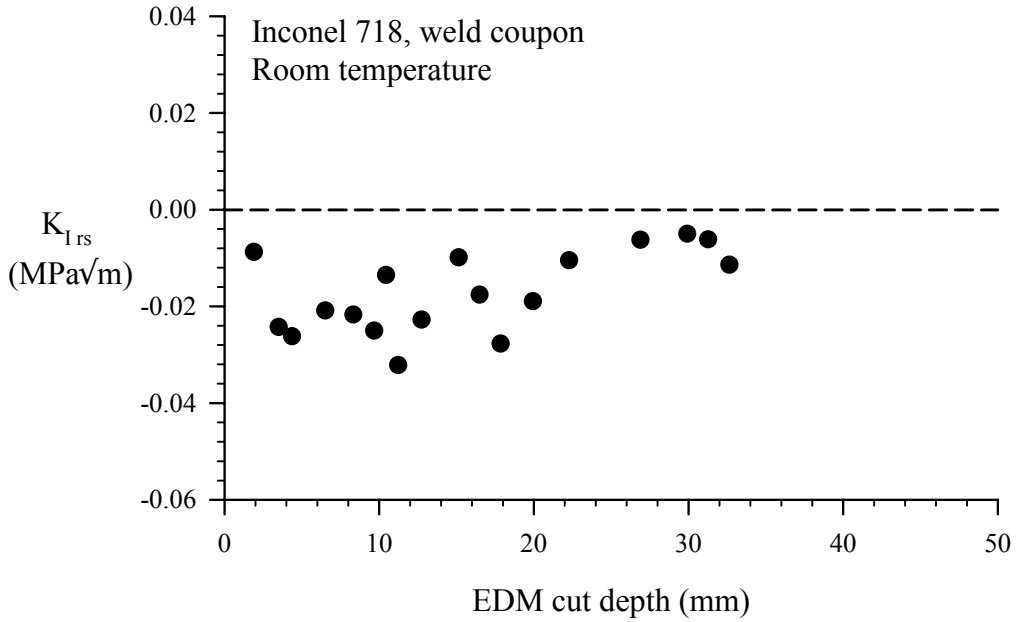

Figure 21. Residual-stress-induced crack-tip stress intensity factors determined from compliance-cut test.

Apparent Fracture Toughness Results[3]

Following fatigue crack growth testing, specimens were loaded to failure in order to measure the relative material toughness. Because these toughness tests were not performed in accordance with standard procedures for fracture toughness, the toughness values obtained may be of limited value. However, these data do permit a relative comparison of the weld metal and base metal properties. Specimens were pre-cracked at K_{max} values no greater than 50% of the toughness values. Toughness tests were performed in displacement control and specimens were loaded at a rate of 1.27 mm/minute (0.05 inch/minute). In all cases, specimens exhibited ductile behavior such that specimens maintained a significant load-carrying capability following the peak load.

The results of the toughness tests are shown in Figure 22a. Because these values were determined from non-standard test procedures, it is more useful to consider the reduction in toughness relative to the base metal value. The normalized toughness values are plotted in Figure 22b. The base metal specimens for both alloys produced the highest toughness values, and the toughness values decreased for starter notch locations closer to the weld center. In other words, the specimen with the starter notch in the center of the weld nugget resulted in the lowest toughness value. By comparing the two alloys, it appears that the toughness of Inconel 718 is most affected by the weld, *i.e.*, the weld metal specimen of Inconel 718 exhibited a toughness of only 46.2% of the base metal while the corresponding CRES 321 value was 69.3% of the base metal value. However, the absolute toughness of Inconel 718 base metal is approximately 50% greater than the CRES 321, so both alloys have nearly the same absolute value of toughness at the weld center (K_{app} = 79 MPa√m). Based on these results, the toughness advantage of Inconel 718 would likely be nullified by the weld repair process.

[3] Here an apparent fracture toughness (K_{app}) determination was conducted. Strict linear-elastic fracture criteria could not be maintained, thus the apparent toughness values should be used for relative comparisons only.

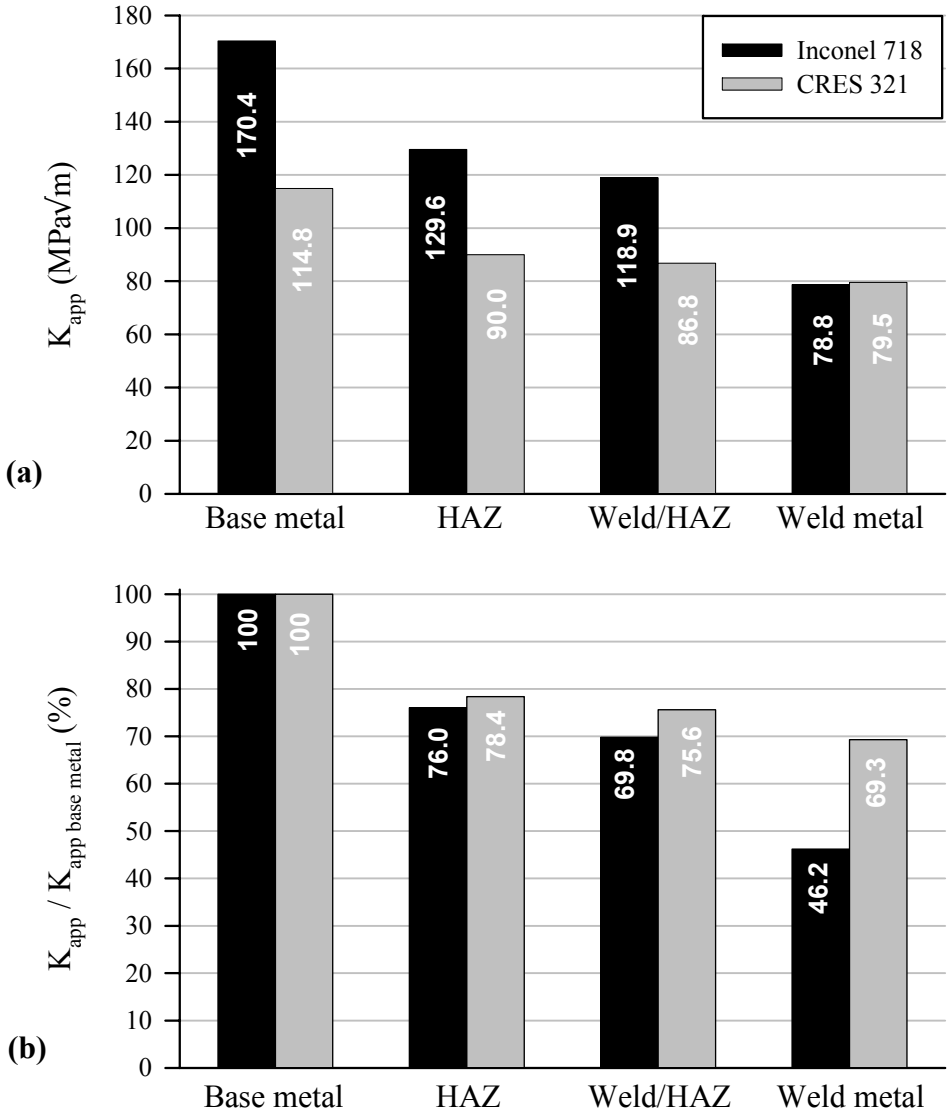

Figure 22. Apparent toughness values for both alloys are shown for cryogenic test temperature (-196°C). (a) Absolute values. (b) Values normalized with base metal toughness.

Summary

A series of fatigue crack growth tests were conducted to characterize the crack growth rate properties of Inconel 718 and CRES 321 sheet that were welded by the MSFC repair process. Carefully chosen constant-K_{max} FCG tests were used to obtain intrinsic (closure-free) crack growth data. Fatigue crack growth was conducted at room and cryogenic (-196°C) temperatures. Inconel 718 welds exhibited lower crack growth rates compared to the base metal, for both ambient and cryogenic temperatures. Welded CRES 321 specimens were found to have slightly higher crack growth rates (relative to the base metal) at ambient temperature. At cryogenic temperature, CRES 321 parent and welded materials exhibited similar fatigue crack growth rates. A compliance-cut method was used to assess the influence of weld residual stress on crack-tip driving force. For cracks propagating at the weld/HAZ boundary and oriented parallel to the direction of the weld, results indicated that residual stresses are compressive and small, resulting in a small reduction in crack-tip stress intensity (K_{Irs} = -0.2 MPa√m). It should be noted that additional

testing would be required to quantify the effects of residual stress. Experimental results show that the FCG characteristics are not significantly affected by residual stresses, but the hardness data for welded Inconel 718 show a significant reduction in hardness, relative to the base metal, suggesting that mechanical properties are likely affected. Toughness testing of the weld repair region suggests that the fracture properties of both Inconel 718 and CRES 321 are reduced compared to the parent material.

References

1. "Standard Test Method for Measurement of Fatigue Crack Growth Rates," *Annual Book of ASTM Standards*, Vol. 3.01, E647, American Society for Testing and Materials, West Conshohocken, PA, 2001.

2. W. F. Deans, C. B. Jolly, W. A. Poyton, and W. Watson, "A Strain Gauging Technique for Monitoring Fracture Mechanics Specimens During Environmental Testing," *Strain*, Volume 13, 1977, pp. 152-154.

3. R. S. Piascik, J. C. Newman, Jr., and J. H. Underwood, "The Extended Compact Tension Specimen," *Fatigue and Fracture of Engineering Materials and Structures*, Volume 20, 1997, pp. 559-563.

4. S. W. Smith and R. S. Piascik, "An Indirect Technique for Determining Closure-Free Fatigue Crack Growth Behavior," *Fatigue Crack Growth Thresholds, Endurance Limits, and Design, ASTM STP 1372*, J.C. Newman, Jr. and R.S. Piascik, Eds., American Society for Testing and Materials, West Conshohocken, PA, 2000, pp. 109-122.

5. J. A. Newman and R. S. Piascik, "Plasticity and Roughness Closure Interactions Near the Fatigue Crack Growth Threshold," *Fatigue and Fracture Mechanics: 33rd Volume, ASTM STP 1417*, W.G. Reuter and R.S. Piascik, Eds., ASTM International, West Conshohocken, PA, 2002, pp. 617-630.

6. S. J. Maddox, Fatigue Strength of Welded Structures, 2nd Edition, Abington Publishing, Cambridge, England, 1991.

7. J. C. Newman, Jr., "Analyses of Fatigue Crack Growth and Closure Near Threshold Conditions for Large-Crack Behavior," NASA/TM-1999-209133, April 1999.

8. H. J. Schindler, "Experimental Determination of Crack Closure by the Cut Compliance Technique," *Advances in Fatigue Crack Closure Measurement and Analysis: Second Volume, ASTM STP 1343*, R.C. McClung and J.C Newman, Jr., Eds., American Society for Testing and Materials, West Conshohocken, PA, 1999, pp. 175-187.

REPORT DOCUMENTATION PAGE

Form Approved
OMB No. 0704-0188

1. REPORT DATE *(DD-MM-YYYY)*	2. REPORT TYPE	3. DATES COVERED *(From - To)*
01- 08 - 2004	Technical Memorandum	

4. TITLE AND SUBTITLE

A Comparison of Weld-Repaired and Base Metal for Inconel 718 and CRES 321 at Cryogenic and Room Temperatures

5a. CONTRACT NUMBER

5b. GRANT NUMBER

5c. PROGRAM ELEMENT NUMBER

6. AUTHOR(S)

Newman, John A.; Smith, Stephen W.; Willard, Scott A.; and Piascik, Robert S.

5d. PROJECT NUMBER

5e. TASK NUMBER

5f. WORK UNIT NUMBER

23-104-08-41

7. PERFORMING ORGANIZATION NAME(S) AND ADDRESS(ES)

NASA Langley Research Center
Hampton, VA 23681-2199

U.S. Army Research Laboratory
Vehicle Technology Directorate
NASA Langley Research Center
Hampton, VA 23681-2199

8. PERFORMING ORGANIZATION REPORT NUMBER

L-19043

9. SPONSORING/MONITORING AGENCY NAME(S) AND ADDRESS(ES)

National Aeronautics and Space Administration
Washington, DC 20546-0001
and U.S. Army Research Laboratory
Adelphi, MD 20783-1145

10. SPONSOR/MONITOR'S ACRONYM(S)

NASA

11. SPONSOR/MONITOR'S REPORT NUMBER(S)

NASA/TM-2004-213253 ARL-TR-3266

12. DISTRIBUTION/AVAILABILITY STATEMENT

Unclassified - Unlimited
Subject Category 26
Availability: NASA CASI (301) 621-0390 Distribution: Standard

13. SUPPLEMENTARY NOTES

An electronic version can be found at http://techreports.larc.nasa.gov/ltrs/ or http://ntrs.nasa.gov

14. ABSTRACT

Fatigue crack growth tests were conducted to characterize the performance of Inconel 718 and CRES 321 welds, weld heat-affect-zone and parent metal at room temperature laboratory air and liquid nitrogen (-196°C) environments. The results of this study were required to predict the damage tolerance behavior of proposed orbiter main engine hydrogen fuel liner weld repairs. Experimental results show that the room and cryogenic temperature fatigue crack growth characteristics of both alloys are not significantly degraded by the weld repair process. Both Inconel 718 and CRES 321 exhibited lower apparent toughness within the weld repair region compared to the parent metal.

15. SUBJECT TERMS

Fatigue crack growth; Inconel 718; CRES 321; Cryogenic; Weld repair; Residual stress; Fuel liner

16. SECURITY CLASSIFICATION OF:			17. LIMITATION OF ABSTRACT	18. NUMBER OF PAGES	19a. NAME OF RESPONSIBLE PERSON
a. REPORT	b. ABSTRACT	c. THIS PAGE			STI Help Desk (email: help@sti.nasa.gov)
					19b. TELEPHONE NUMBER *(Include area code)*
U	U	U	UU	27	(301) 621-0390